NV-based quantum memories coupled to photonic integrated circuits

Sara Mouradian[a], Tim Schröder[a], Jiabao Zheng[a,b], Tsung-Ju Lu[a], Hyeongrak Choi[a], Noel Wan[a], Michael Walsh[a], Eric Bersin[a], and Dirk Englund[a]

[a]Massachusetts Institute of Technology, Cambridge MA, USA
[b]Columbia University, New York, New York 10027, United States

ABSTRACT

The negatively charged nitrogen vacancy (NV) center in diamond is a promising solid-state quantum memory. However, developing networks comprising such quantum memories is limited by the fabrication yield of the quantum nodes and the collection efficiency of indistinguishable photons. In this letter, we report on advances on a hybrid quantum system that allows for scalable production of networks, even with low-yield node fabrication. Moreover, an NV center in a simple single mode diamond waveguide is shown in simulation and experiment to couple well to a single mode SiN waveguide with a simple adiabatic taper for optimal mode transfer. In addition, cavity enhancement of the zero phonon line of the NV center with a resonance coupled to the waveguide mode allows a simulated >1800 fold increase in the collection of photon states coherent with the state of the NV center into a single frequency and spatial mode.

Keywords: Quantum Information; Photonic Circuit; Integration; Quantum Memory; Wide Band-Gap Materials; Waveguides; Modulators; Diamond

1. INTRODUCTION

Quantum computation and communication systems leverage the unique properties of quantum physics to surpass their classical counterparts in certain applications. Quantum algorithms provide speed-ups in solving problems which are classically intractable, such as prime factoring[1] and graph search.[2] Quantum communication systems enable physics-based security over long distances provided quantum repeaters exist at intermediate nodes.[3] Both quantum computation and long-distance quantum communication systems require a network of entangled logical quantum bits (qubits) which can be individually controlled and read out.[4] However, building and maintaining these entangled network states is challenging due to the many decoherence pathways any experimental system encompasses. Over the past decade, there has been rapid progress in developing theoretical platforms for building high-fidelity entangled networks using stationary qubits connected via photons, even in the presence of state decoherence.[5–8] Though many experimental platforms are being pursued, the successful scaling of any platform to tens, or eventually hundreds, of optically connected qubits will likely require photonic integrated circuits (PICs) for their compact footprint, low loss, and phase stability. This is a direct parallel to the classical computing revolution that was enabled by the advent of integrated circuits.

In a PIC architecture, solid-state qubits are a clear choice for their ease of manipulation. One promising solid-state quantum memory with second-scale spin coherence times is the negatively charged nitrogen vacancy (NV) center in diamond.[9,10] Its electronic spin state can be optically initialized, manipulated, measured,[11] and mapped onto nearby auxiliary nuclear memories,[12] allowing for increased coherence time and quantum error correction. Quantum network protocols based on these unique qualities have been proposed,[13,14] and entanglement generation and state teleportation between two spatially separated quantum memories have been demonstrated.[15–17] Translating such entanglement techniques into an on-chip architecture promises scalability, but requires near-unity-yield fabrication of high quality solid state quantum memories efficiently coupled to low-loss single mode waveguides. In this paper, we will present recent progress on integrating solid state quantum memory bits into a PIC photonic processor, and discuss the advances necessary to demonstrate on-chip entanglement.

Further author information:
D.E.: E-mail: englund@mit.edu
S.M.: E-mail: smouradi@mit.edu

2. HYBRID PHOTONIC CIRCUITS

Advances in the nanofabrication of diamond over the last decade[18] have enabled the fabrication of simple photonic networks from bulk diamond,[19] diamond-on-insulator[20,21] substrates, and in fiber based architectures.[?,22] However, patterning in diamond is challenging,[23,24] and the creation of a single NV at a pre-defined location is inherently low yield ($\sim 1 - 3\%$ even with apertured implantation[25–27]) due to the stochastic process of NV creation. Unfortunately, the fabrication overhead needed to build an all-diamond monolithic network scales exponentially with the number of nodes, and thus is prohibitive with such low node yields. For example, the successful fabrication of a 5-node network with 1% node yield would require on average 10^5 fabrication attempts. On the other hand, the fabrication overhead needed for a hybrid approach which decouples the fabrication of nodes from the fabrication of the PIC components scales linearly with the number of necessary nodes. In contrast to the monolithic approach, the successful fabrication of a 5-node network with 1% node yield requires only 500 node fabrication attempts. Furthermore, a hybrid approach will take advantage of strong industrial fabrication development in wide band-gap semiconductors to fabricate high-throughput PICs. Therefore, we argue that a hybrid approach is necessary to scale current systems from two nodes to the tens, or even hundreds, of nodes necessary to show quantum advantages over classical systems.

In this hybrid architecture, quantum nodes based on NV centers in short, single mode waveguides—possibly with cavities, as discussed in Sec. 3—are fabricated in arrays. These arrays are characterized in a confocal setup to evaluate NV positioning and alignment with respect to the waveguide (or cavity) mode. The quantum properties of the NV, such as the spin coherence time and optical linewidth, can also be measured at this stage. After pre-characterization, only the best structures are integrated into a high quality PIC fabricated into a wide bandgap semiconductor such as Silicon Nitride (SiN) or Aluminum Nitride (AlN).[28] The essential pre-characterization and selection step guarantees that every node in the PIC contains a single NV well-coupled to the optical mode with the desired spectral and spin properties. It also decouples the fabrication of each of the nodes from the desired network architecture and connectivity.
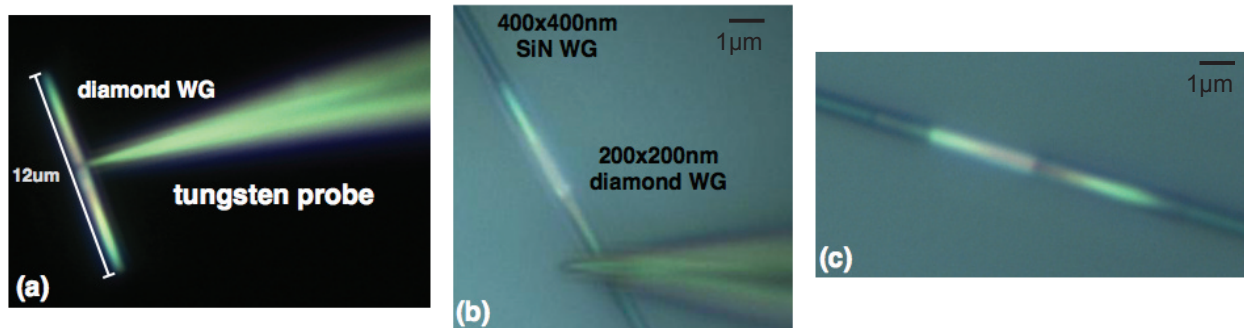

Figure 1. The integration process. (a) White light microscope image of a 12 µm diamond µWG held at the center by a tungsten probe. (b) Placement of a µWG into a SiN PIC. (c) Microscope image of a typical placement showing alignment precision of tens of nanometers between the diamond µWG and the SiN PIC.

The keystone step in creating a hybrid quantum network is the integration of the diamond micro-waveguide (µWG) into the PIC backbone in a controllable and repeatable way. The full hybrid-PIC fabrication method is illustrated in Fig. 1. Arrays of quantum nodes—in this case simple $0.2 \times 0.2 \times 12$ µm single mode diamond micro-waveguides (µWGs) with tapered ends—are fabricated in a 200 nm thick diamond membrane and characterized under a confocal microscope to determine the location of single NVs via spectral and autocorrelation measurements. A single tungsten probe tip (~ 500 nm tip radius) is used to pick up the desired µWG. Electrostatic forces cause the adhesion between the µWG and the tungsten tip. The strength of the adhesion can be changed through surface termination, for example by a solvent clean of the tungsten tip. An elevated tungsten

tip with a single picked nanowire is shown in Fig. 1(a). The nanowire is aligned to the integration region in a high-NA microscope, as seen in Fig. 1(b). Again, the adhesion between the nanowire and the PIC depends on electrostatic forces, and thus is heavily influenced by the surface termination of the PIC. We have found that ashing the PIC surface in oxygen plasma for 5 minutes at 100 W plasma power within one hour of integration increases adhesion, allowing for a smooth and repeatable integration process. Fig. 1(c) shows a diamond µWG integrated into a SiN PIC.

A simple tapered diamond waveguide structure effectively couples light from an NV at the mode maximum into the PIC waveguide. A snapshot of the mode in the system is shown in Fig 2(a). The first image in Fig. 2(a) illustrates that the NV emits preferentially (86%) into the single mode of the diamond waveguide. The third image in Fig. 2(a) illustrates that with optimized tapers 95% of the light collected into the diamond waveguide mode is adiabatically transferred to the underlying PIC waveguide mode due to tapers in both the PIC and diamond waveguides. With optimal tapers and optimal NV placement and orientation, 82% of the light emitted by the NV will be coupled into the PIC.[28] This is a broadband effect, and increases the collection across the NV spectrum (~630 nm-750 nm).

To illustrate the efficient optical coupling from an NV into the underlying PIC, four µWGs were placed onto a single SiN PIC. The state of each NV could be controlled via optical pulses delivered through a confocal setup (NA = 0.9), and microwave pulses delivered through a thin wire loop. Light was collected via the confocal setup, as well as through the waveguide into a lensed single mode fiber. In both cases, the collected light was sent either to an avalanche photodiode (APD), Hanbury-Brown-Twiss setup, or spectrometer to measure count rate, photon statistics, and spectrum, respectively. We were able to collect 3.5 times more light into one direction of the waveguide[28] in the system with best NV orientation and position with respect to the waveguide mode, even with non-optimal tapers which taper only to 100 nm, and non-optimal NV placement.
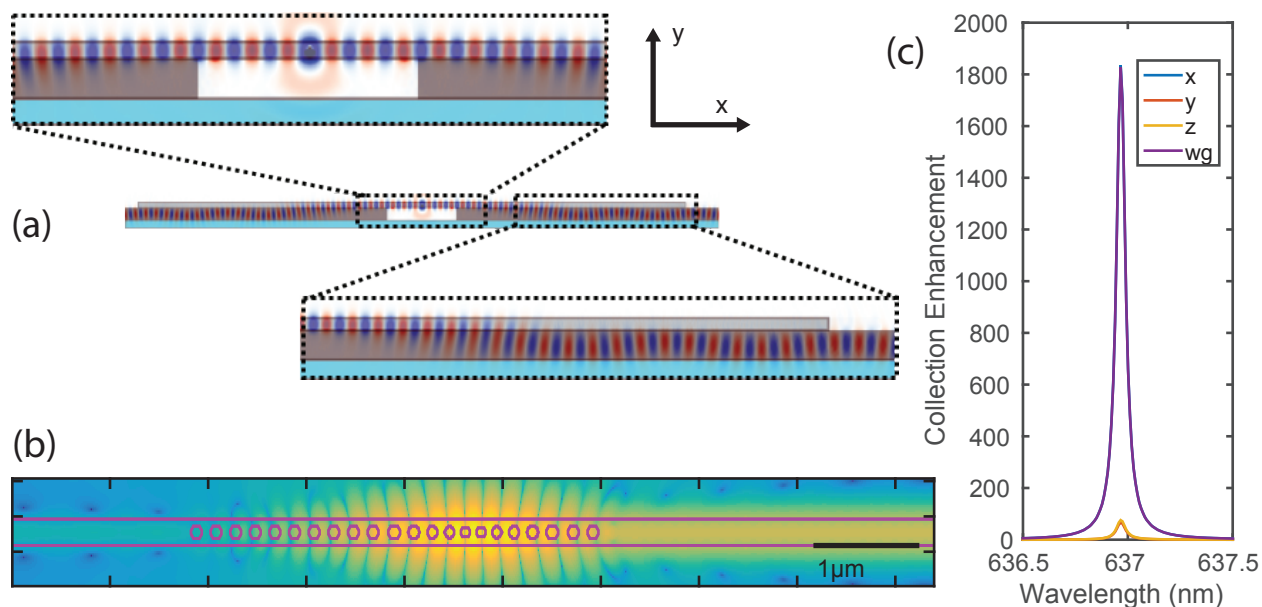

Figure 2. Coupling from the NV to the underlying PIC. (a) An optimally placed NV in a suspended 200×200 nm diamond µWG couples well into the single optical mode. Tapers in the diamond waveguide and the underlying PIC allow light to couple efficiently between the two waveguides. (b) Field profile ($\log_{10}|E|^2$) of a diamond photonic crystal nanobeam cavity loaded into one direction of the waveguide mode. (c) Collection enhancement into the x,y,z planes, as well as one direction of the waveguide for an optimally placed NV. This is normalized to the collection expected for an NV optimally placed in an unpatterned diamond µWG.

3. PURCELL ENHANCEMENT

Creating hybrid quantum systems separates the stochastic, and thus low-yield, creation of solid state qubits from the high yield fabrication of the underlying PIC backbones and allows the physical scaling from one qubit to multiple qubits optically connected in the same PIC. However, it is also necessary to entangle arbitrary groups of these integrated qubits to build a quantum repeater or quantum information processor. In addition, to successfully perform a computation or transmit information, the necessary single and multi-qubit gates must be executed within the coherence time of the entangled state. As discussed in Sec. 2, the simple unpatterned diamond µWG provides a broadband increase in collection efficiency for NV centers well coupled to the single optical mode of the diamond waveguide compared to a non-patterned diamond. However, even at low temperatures, the NV center suffers from strong interactions with phonon modes in the diamond lattice, and only ∼3% of the photons emitted by an NV center enable direct coherent spin state readout. For the remaining 97%, an interaction with one or more phonons erases that information. Thus, the simple enhancement in collection efficiency over the broad spectrum of the NV will not achieve an entanglement rate larger than the spin decoherence rate.[15] For that, the emission at the zero-phonon line (ZPL)–the only transition which emits photon states which are entangled with the NV spin state–must be enhanced with an optical cavity via the Purcell effect.[29,30]

For the hybrid system introduced in Sec. 2, it is important that the cavity is loaded into the waveguide mode so that the light can be effectively collected into a single optical mode. To that end, we have designed nanobeam diamond cavities which enhance the ZPL emission, and are loaded into one direction of the waveguide mode. A bandgap at the NV ZPL wavelength (637 nm) is created by periodic holes ($a = 215$ nm) in a 250×230 nm diamond µWG. A defect in the photonic crystal, enabling 3d light capture, is created by a 5-hole linear taper of the period down to 161 nm, while the ratio between the radius and the period is kept constant ($r/a = 0.28$). The simulated unloaded quality factor (Q)—with >10 holes on either side of the cavity region to minimize coupling into the waveguide mode—is >100,000. To increase coupling into the underlying PIC, the cavity is loaded into one direction of the diamond µWG by removing holes on one side of the cavity, as illustrated in Fig. 2. In this case, the loaded Q is >12,000, with a ∼1800 times enhancement of collection into one direction of a single diamond waveguide mode over an unpatterned diamond waveguide in simulation. The loaded mode profile and the spectra collection enhancement into the single mode of the diamond µWG are shown in Fig. 2(b,c) respectively. The diamond µWG is tapered adiabatically as in the unpatterned µWG to provide high coupling to a single mode in the underlying PIC. This increased coupling of NV ZPL photons coherent with the spin state into a single guided frequency and spatial mode due to Purcell enhancement of the ZPL, and engineered loading into the waveguide mode will increase entanglement rates to well below the spin decoherence rate.

4. CONCLUSIONS

In this letter, we have addressed two challenges in scaling a quantum system from one or two nodes to many entangled nodes. A hybrid fabrication approach decouples the low-yield node fabrication and allows for the assembly of a final system in which every qubit is of high quality, and is connected to the PIC architecture; it was recently shown that tunable PICs can produce nearly perfect optical unitary transformations despite imperfect fabrication.[31,32]

Secondly, a waveguide-loaded cavity design was introduced that increased the collection efficiency of indistinguishable photons in a single frequency and spatial mode, which will increase entanglement rates to well above the spin decoherence rate, allowing multiple entanglement operations during a single spin coherence time. We believe that these two advancements will enable the scaling of quantum systems, but there are still many engineering challenges to be overcome. On-chip microwave lines to every node with low cross talk are necessary for efficient state preparation; on-chip laser delivery to many nodes with fast switching is necessary for parallel optical addressing; and finally, fast classical processing of photon detection events and feedback is required for the successful implementation of many entanglement events within the coherence time. All of these goals are compatible with an on-chip hybrid system and thus the results presented here will enable scalable quantum systems.

ACKNOWLEDGMENTS

REFERENCES

[1] P. W. Shor, "Algorithms for quantum computation: Discrete logarithms and factoring," in *Foundations of Computer Science, 1994 Proceedings., 35th Annual Symposium on*, pp. 124–134, IEEE, 1994.

[2] L. K. Grover, "A fast quantum mechanical algorithm for database search," in *Proceedings of the twenty-eighth annual ACM symposium on Theory of computing*, pp. 212–219, ACM, 1996.

[3] H.-J. Briegel, W. Dür, J. I. Cirac, and P. Zoller, "Quantum repeaters: The role of imperfect local operations in quantum communication," *Phys. Rev. Lett.* **81**, pp. 5932–5935, 1998.

[4] M. A. Nielsen and I. Chuang, *Quantum computation and quantum information*, Cambridge University Press, Cambridge, U.K; New York, 2000.

[5] J. I. Cirac, P. Zoller, H. J. Kimble, and H. Mabuchi, "Quantum State Transfer and Entanglement Distribution among Distant Nodes in a Quantum Network," *Phys. Rev. Lett.* **78**(16), pp. 3221–24, 1997.

[6] H. Kimble, "The quantum internet," *Nature* **453**, pp. 1023–30, 2008.

[7] T. Northup and R. Blatt, "Quantum information transfer using photons," *Nature Photon.* **8**(53), pp. 356–63, 2014.

[8] S. D. Barrett and P. Kok, "Efficient high-fidelity quantum computation using matter qubits and linear optics," *Phys. Rev. A* **71**, p. 060310, Jun 2005.

[9] P. C. Maurer, G. Kucsko, C. Latta, L. Jiang, N. Y. Yao, S. D. Bennett, F. Pastawski, D. Hunger, N. Chisholm, M. Markham, D. J. Twitchen, J. I. Cirac, and M. D. Lukin, "Room-temperature quantum bit memory exceeding one second," *Science* **336**(6086), pp. 1283–6, 2012.

[10] N. Bar-Gill, L. M. Pham, A. Jarmola, D. Budker, and R. L. Walsworth, "Solid-state electronic spin coherence time approaching one second," *Nat. Commun.* **4**, p. 1743, 2013.

[11] P. Neumann, J. Beck, M. Steiner, F. Rempp, H. Fedder, P. R. Hemmer, J. Wrachtrup, and F. Jelezko, "Single-shot readout of a single nuclear spin," *Science* **329**(5991), pp. 542–544, 2010.

[12] M. V. G. Dutt, L. Childress, L. Jiang, E. Togan, J. Maze, F. Jelezko, A. S. Zibrov, P. R. Hemmer, and M. D. Lukin, "Quantum register based on individual electronic and nuclear spin qubits in diamond," *Science* **316**(5829), pp. 1312–6, 2007.

[13] L. Childress, J. M. Taylor, A. S. Sorensen, and M. D. Lukin, "Fault-tolerant quantum repeaters with minimal physical resources and implementations based on single-photon emitters," *Phys. Rev. A* **72**, p. 052330, 2005.

[14] K. Nemoto, M. Trupke, S. J. Devitt, A. M. Stephens, B. Scharfenberger, K. Buczak, T. Nöbauer, M. S. Everitt, J. Schmiedmayer, and W. J. Munro, "Photonic architecture for scalable quantum information processing in diamond," *Phys. Rev. X* **4**, p. 031022, Aug 2014.

[15] W. Pfaff, B. Hensen, H. Bernien, S. van Damm, M. Blok, T. Taminiau, M. Tiggelman, R. Schouten, M. Markham, D. J. Twitchen, and R. Hanson, "Unconditional quantum teleportation between distant solid-state quantum bits," *Science* **10**(1126), p. 1253512, 2014.

[16] H. Bernien, B. Hensen, W. Pfaff, G. Koolstra, M. S. Blok, L. Robledo, T. H. Taminiau, M. Markham, D. J. Twitchen, L. Childress, and R. Hanson, "Heralded entanglement between solid-state qubits separated by three metres," *Nature* **497**(7447), pp. 86–90, 2013.

[17] B. Hensen, H. Bernien, A. Dréau, A. Reiserer, N. Kalb, M. Blok, J. Ruitenberg, R. Vermeulen, R. Schouten, C. Abellán, *et al.*, "Loophole-free bell inequality violation using electron spins separated by 1.3 kilometres," *Nature* **526**(7575), pp. 682–686, 2015.

[18] T. Schröder, S. L. Mouradian, J. Zheng, M. E. Trusheim, M. Walsh, E. H. Chen, L. Li, I. Bayn, and D. Englund, "Quantum nanophotonics in diamond [invited]," *JOSA B* **33**(4), pp. B65–B83, 2016.

[19] I. Bayn, S. Mouradian, L. Li, J. A. Goldstein, T. Schröder, J. Zheng, E. H. Chen, O. Gaathon, M. Lu, A. Stein, C. A. Ruggiero, J. Salzman, R. Kalish, and D. Englund, "Fabrication of triangular nanobeam waveguide networks in bulk diamond using single-crystal silicon hard masks," *Applied Physics Letters* **105**, p. 211101, 2014.

[20] P. Rath, N. Gruhler, S. Khasminskaya, C. Nebel, C. Wild, and W. Pernice, "Waferscale nanophotonic circuits made from diamond-on-insulator substrates," *Optics express* **21**(9), pp. 11031–11036, 2013.

[21] M. Gould, S. Chakravarthi, I. R. Christen, N. Thomas, S. Dadgostar, Y. Song, M. L. Lee, F. Hatami, and K.-M. C. Fu, "Large-scale gap-on-diamond integrated photonics platform for nv center-based quantum information," *JOSA B* **33**(3), pp. B35–B42, 2016.

[22] R. N. Patel, T. Schröder, N. Wan, L. Li, S. L. Mouradian, E. H. Chen, and D. R. Englund, "Efficient photon coupling from a diamond nitrogen vacancy center by integration with silica fiber," *Light: Science & Applications* **5**(2), p. e16032, 2016.

[23] L. Li, I. Bayn, M. Lu, C.-Y. Nam, T. Schröder, A. Stein, N. C. Harris, and D. Englund, "Nanofabrication on unconventional substrates using transferred hard masks," *Scientific reports* **5**, 2015.

[24] B. Khanaliloo, M. Mitchell, A. C. Hryciw, and P. E. Barclay, "High-q/v monolithic diamond microdisks fabricated with quasi-isotropic etching," *Nano letters* **15**(8), pp. 5131–5136, 2015.

[25] M. Schukraft, J. Zheng, T. Schröder, S. Mouradian, M. Walsh, M. Trusheim, H. Bakhru, and D. Englund, "Invited article: Precision nanoimplantation of nitrogen vacancy centers into diamond photonic crystal cavities and waveguides," *APL Photonics* **1**(2), p. 020801, 2016.

[26] D. Scarabelli, M. E. Trusheim, O. Gaathon, D. R. Englund, and S. J. Wind, "Nanoscale engineering of closely-spaced electronic spins in diamond," *Nano Letters* , 2016.

[27] I. Bayn, E. H. Chen, M. E. Trusheim, L. Li, T. Schröder, O. Gaathon, M. Lu, A. Stein, M. Liu, K. Kisslinger, *et al.*, "Generation of ensembles of individually resolvable nitrogen vacancies using nanometer-scale apertures in ultrahigh-aspect ratio planar implantation masks," *Nano letters* **15**(3), pp. 1751–1758, 2015.

[28] S. L. Mouradian, T. Schröder, C. B. Poitras, L. Li, J. Goldstein, E. H. Chen, M. Walsh, J. Cardenas, M. L. Markham, D. J. Twitchen, M. Lipson, and D. Englund, "Scalable integration of long-lived quantum memories into a photonic circuit," *Phys. Rev. X* **5**, p. 031009, Jul 2015.

[29] L. Li, T. Schröder, E. H. Chen, M. Walsh, I. Bayn, J. Goldstein, O. Gaathon, M. E. Trusheim, M. Lu, J. Mower, *et al.*, "Coherent spin control of a nanocavity-enhanced qubit in diamond," *Nature communications* **6**, 2015.

[30] A. Faraon, P. E. Barclay, C. Santori, K.-M. C. Fu, and R. G. Beausoleil, "Resonant enhancement of the zero-phonon emission from a colour centre in a diamond cavity," *Nature Photonics* **5**(5), pp. 301–305, 2011.

[31] J. Mower, N. C. Harris, G. R. Steinbrecher, Y. Lahini, and D. Englund, "High-fidelity quantum state evolution in imperfect photonic integrated circuits," *Phys. Rev. A* **92**, p. 032322, Sep 2015.

[32] D. A. Miller, "Perfect optics with imperfect components," *Optica* **2**(8), pp. 747–750, 2015.